2024 IEEE/RSJ International Conference on Intelligent Robots and Systems (IROS)
October 14-18, 2024. Abu Dhabi, UAE

Navigated Locomotion and Controllable Splitting of a Microswarm in a Complex Environment

Yuezhen Liu[1,2,†], Guangjun Zeng[1,†], Xingzhou Du[1,2], Kaiwen Fang[1,2], and Jiangfan Yu[1,2]

Abstract— **Reconfigurable microswarms have received extensive attention recently. In this work, we propose a control strategy for a ribbon-like swarm to perform navigated locomotion with a stable pattern, and perform controllable splitting into double subswarms to reach two targets simultaneously. Two different behaviors of the ribbon-like swarm are firstly investigated, i.e., locomotion with a stable pattern, and controllable splitting. The two behaviors of the ribbon-like swarm are realized based on different aspect ratio of the swarm. Subsequently, we propose a morphology controller to keep the aspect ratio of the swarm within a desired range. The morphology controller consists of a feedforward controller and a PD controller. The feedforward controller containing a fitted model, and a fuzzy logic controller for online compensation of the model error. The control strategy combining the morphology planning, morphology controller, path planning, and motion controller is developed. Using the proposed control strategy, the ribbon-like swarm can be navigated to follow a desired path with a stable pattern while avoiding obstacles, and finally perform controllable splitting into double subswarms to reach two predefined targets simultaneously.**

I. Introduction

Microrobots have received extensive attention recently due to their potential applications in embolization, biosensing, micromanipulation, and targeted cargo delivery [1], [2], [3], [4], [5]. Various microrobots have been widely investigated, such as soft microrobots [6], [7], [8], helical-shaped microswimmers [9], [10], [11], and bio-hybrid microrobots [12], [13], [14]. Among them, microswarms serve as promising candidates, since they can perform multitype shape reconfigurations to adapt to different environments [15], [16], [17], and microswarms can carry a larger volume of cargo compared to individual microrobots.

Adaptive control strategies and advanced navigation algorithms are critical for the precise locomotion of microrobots in complex environments. Based on model predictive control, a spore-based microrobot can reach the target in an environment with obstacles by following an optimal path generated using PSO algorithm [18]. A control strategy combining proxy-based sliding control and optimal Bidirectional RRT* is developed, and a helical microswimmer can perform precise locomotion to avoid obstacles in 3-D space using the strategy [19]. A spherical microrobot is capable of avoiding a single mobile obstacle based on artificial potential field method and fuzzy logic controller [20]. These methods mainly focus on the motion control of microrobots with rigid body, and strategies have also been proposed for the control and navigation of reconfigurable microswarms. A control strategy containing a LQI controller and an extended state observer is designed for the motion control of a vortex-like swarm [21]. A vortex-like swarm can also avoid dynamic obstacles in a micromaze using a radar-based control strategy [22]. Based on EB-RRT* path planning method and GA-LQR motion controller, a ribbon-like swarm can track a dynamic target while passing obstacles [23]. These control strategies are developed for the motion control of microswarms, and the morphology control of the microswarms are not investigated. The morphology control of an elliptical swarm has been studied [24], but the influence of the morphology of the swarm on its locomotion still needs further investigations. A ribbon-like swarm can perform controllable splitting [25], but the control process is conducted manually. Therefore, a control strategy needs to be developed for the automatic splitting of the ribbon-like swarm, in order to increase the compatibility of the controllable splitting in complex environments.

In this work, we propose a control strategy to automatically navigate the ribbon-like swarm to perform locomotion with a stable pattern while avoiding obstacles, and perform controllable splitting into double swarms to reach two targets simultaneously. We firstly investigate the influence of the morphology of the ribbon-like swarm on the two behaviors of it, i.e., locomotion with a stable pattern, and controllable splitting. If the aspect ratio of the ribbon-like swarm is kept at a small value, the swarm can perform locomotion with a stable pattern, even when the moving direction of the swarm changes swiftly. If the aspect ratio of the ribbon-like swarm is kept at a large value, the swarm is capable of performing controllable splitting into multiple subswarms with a sudden change of the moving direction. The relationship between the number of the subswarms after splitting and the aspect ratio of the ribbon-like swarm before splitting is obtained. Because the two behaviors of the ribbon-like swarm are determined by its aspect ratio, a morphology controller is subsequently developed to control the aspect ratio of the swarm. The morphology controller consists of a feedforward controller and a PD controller. The feedforward controller

This work was supported in part by the National Key R&D Program of China under Project No. 2022YFA1207100, the National Natural Science Foundation of China under Grant 62103347, Shenzhen Science and Technology Innovation Program under Grant RCBS20210609103155061, Guangdong Basic and Applied Basic Research Foundation under Grant 2023A1515012973 and Grant 2022A1515110499, and in part by Shenzhen Institute of Artificial Intelligence and Robotics for Society. (†Yuezhen Liu and Guangjun Zeng contributed equally to this work.) (Corresponding author: Jiangfan Yu. E-mail: yujiangfan@cuhk.edu.cn)

[1]School of Science and Engineering, The Chinese University of Hong Kong, Shenzhen 518172, China.

[2]Shenzhen Institute of Artificial Intelligence and Robotics for Society (AIRS), Shenzhen 518129, China.

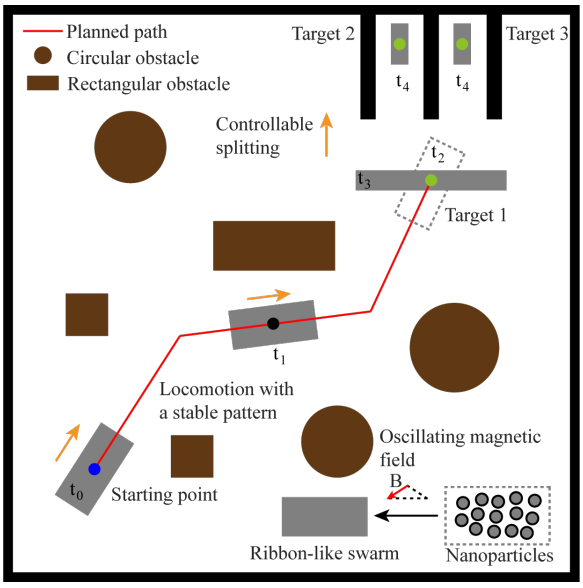

Fig. 1. Generation and automatic navigation of a ribbon-like swarm. The grey rectangles denote the ribbon-like swarms. The orange arrows indicate the moving direction of the swarm. The green dots are the targets, and the brown circles and rectangles represent the obstacles.

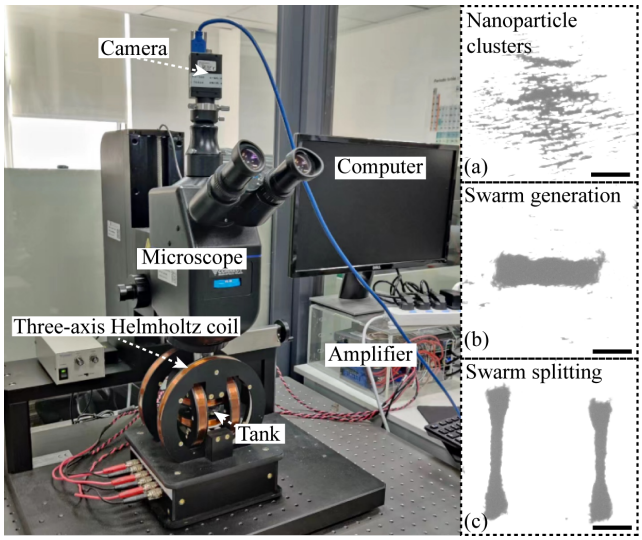

Fig. 2. The experimental system. The three insets (a), (b), and (c) show the nanoparticle clusters, the ribbon-like swarm, and two ribbon-like swarms after splitting, respectively. The scale bar is 500 μm.

contains a fitted model, and a fuzzy logic controller for online compensation of the model error. Using the morphology controller, the aspect ratio of the ribbon-like swarm can be kept within a desired range. The control strategy combining the morphology planning, morphology controller, path planning, and motion controller of the swarm is proposed. Based on the proposed control strategy, the ribbon-like swarm can firstly perform navigated locomotion with a stable pattern when its aspect ratio is small, and subsequently perform controllable splitting into double subswarms when it has a large aspect ratio. Finally, the double subswarms can reach two targets simultaneously.

II. Generation and Automatic Navigation of a Ribbon-like Swarm

Based on the control strategy for automatic navigation of a ribbon-like swarm, the swarm can perform navigated locomotion with a stable pattern in an environment with obstacles, and split into double subswarms to reach two targets simultaneously, as shown in Fig. 1. The ribbon-like swarm is firstly generated from nanoparticles using an oscillating magnetic field. By adding a pitch angle φ and a direction angle θ of the magnetic field, the ribbon-like swarm can perform locomotion in 2-D space, and the oscillating magnetic field can be expressed as [23]:

$$B = \begin{bmatrix} A\cos(\theta)\cos(\varphi)\sin(2\pi ft) - K\sin(\theta) \\ A\sin(\theta)\cos(\varphi)\sin(2\pi ft) + K\cos(\theta) \\ -A\sin(\varphi)\sin(2\pi ft) \end{bmatrix} \quad (1)$$

where A and f are the amplitude and the frequency of the magnetic field, respectively. The field ratio γ is denoted by A/K, and the aspect ratio of the ribbon-like swarm α can be adjusted by tuning the field ratio γ.

III. System Setup

The experimental system used to generate and actuate the ribbon-like swarm is shown in Fig. 2. The three-axis Helmholtz coil is built to generate the oscillating magnetic field. The control strategy is implemented on the computer, and the camera and the microscope are used to obtain the experimental image. To generate the ribbon-like swarm, 3 μl of nanoparticle suspension (3 mg/ml) is firstly added into the tank filled with 0.1% BSA solution, as shown by the nanoparticle clusters in the inset (a) of Fig. 2. A piece of silicon wafer is placed at the bottom of the tank to enhance the image contrast. Subsequently, using the oscillating magnetic field, the ribbon-like swarm is generated, as shown in the inset (b) of Fig. 2. The amplitude and the frequency of the magnetic field is set to 10 mT and 10 Hz, respectively. With a sudden change of the direction angle of the magnetic field, the ribbon-like swarm can split into two subswarms, as shown in the inset (c) of Fig. 2.

IV. Two Different Behaviors of a Ribbon-like Swarm

Herein, we investigate two different behaviors of a ribbon-like swarm, i.e., locomotion with a stable pattern, and controllable splitting. The two behaviors of the swarm can be realized based on different aspect ratio of the swarm.

A. Locomotion of a ribbon-like swarm with a stable pattern

The schematics of the locomotion of a ribbon-like swarm with a stable pattern, and the splitting of the swarm is shown in Fig. 3(a). If the aspect ratio of the ribbon-like swarm is small, the swarm can perform locomotion with a stable pattern, even when its moving direction changes swiftly. For instance, when the aspect ratio of the swarm α is 3.2, as shown in Fig. 3(a), the moving direction of the ribbon-like swarm suddenly changes from 0 degree to 90 degree, but

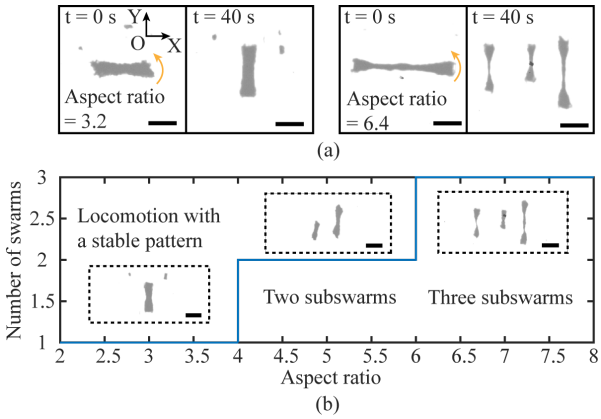

Fig. 3. The schematics of the locomotion of a ribbon-like swarm with a stable pattern, and controllable splitting of the swarm. (a) The locomotion of the ribbon-like swarm with a stable pattern, and splitting of the swarm. (b) The controllable splitting of the ribbon-like swarm. The scale bar is 500 μm.

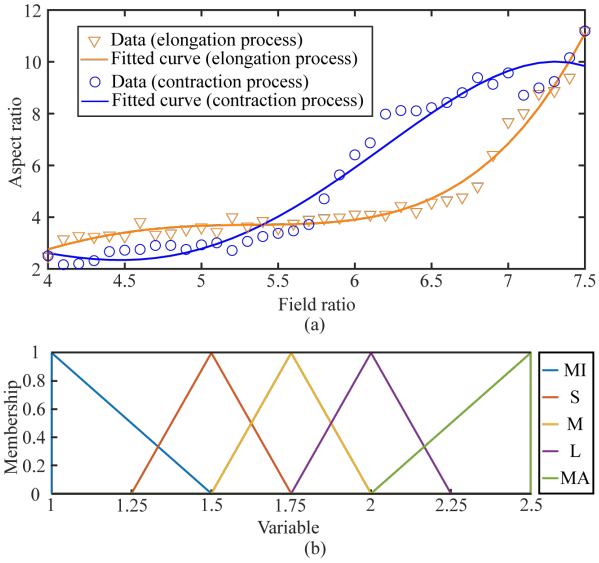

Fig. 4. The schematics of the fitted model to obtain the field ratio to control the swarm, and the membership function of the variables in the fuzzy logic controller. (a) The fitted curve indicating the relationship between the aspect ratio and the field ratio. (b) The membership functions of the variables in the fuzzy logic controller. MI: minimum; S: small; M: middle; L: large; MA: maximum.

the pattern of the ribbon-like swarm remains stable without splitting. In contrast, when the aspect ratio of the swarm is large, e.g., α = 6.4, the moving direction of the swarm changes from 0 degree to 90 degree, and the swarm splits into three parts, as shown in Fig. 3(a). In this case, the instability of the swarm pattern occurs, when the moving direction of the swarm changes swiftly. Therefore, it is necessary to control the aspect ratio of the ribbon-like swarm to be small for the locomotion of the swarm with a stable pattern.

B. Controllable splitting of a ribbon-like swarm

Although the splitting of the ribbon-like swarm indicates the instability of the swarm pattern, the controllable splitting of the ribbon-like swarm has potential to be applied in the field of muti-target delivery using microswarms. For instance, a ribbon-like swarm can split into two subswarms, and the double swarms are capable of reaching two targets simultaneously. In this work, the splitting of the ribbon-like swarm is realized by generating a sudden change of the moving direction of the swarm. When the moving direction of the swarm changes from 0 degree to 90 degree swiftly, the relationship between the number of subswarms after splitting and the aspect ratio of the swarm before splitting is shown in Fig. 3(b). When the aspect ratio of the swarm ranges from 2 to 4, the swarm can perform locomotion with a stable pattern. The number of the swarms after splitting is 2 and 3, when the aspect ratio of the swarm before splitting ranges from 4 to 6 and from 6 to 8, respectively. From Fig. 3(b), the number of subswarms after splitting is based on the aspect ratio of the swarm before splitting. Therefore, in order to obtain controllable number of swarms for muti-target reaching, it is necessary to control the aspect ratio of the ribbon-like swarm within a desired range before the swarm performs splitting.

V. Control Methodology

From Section IV, the control of the aspect ratio of the ribbon-like swarm is necessary for its locomotion with a stable pattern, and controllable splitting. Therefore, we propose a morphology controller to keep the aspect ratio of the ribbon-like swarm within a desired range, and a control strategy containing the morphology controller is proposed for the navigated locomotion and controllable splitting of the ribbon-like swarm.

A. Morphology control of a ribbon-like swarm

The morphology controller for the ribbon-like swarm contains a feedforward controller and a PD controller. The feedforward controller consists of a fitted model to obtain the preliminary field ratio γ_p corresponding to the desired aspect ratio α_d, and a fuzzy logic controller (FLC) to compensate the model error. The fitted model is obtained based on collected experimental data. The fitted curves indicating the relationship between the aspect ratio and the field ratio is shown in Fig. 4(a), and the relationship is different during the elongation and contraction process of the swarm. Based on the relationship, the fitted model can be obtained, which can be expressed as:

$$\gamma_p = \begin{cases} 0.0013759{\alpha_d}^4 - 0.014994{\alpha_d}^3 - 0.20453{\alpha_d}^2 \\ +3.2066\alpha_d - 3.2483, \ \alpha < \alpha_d \\ -0.004839{\alpha_d}^4 + 0.13992{\alpha_d}^3 - 1.4256{\alpha_d}^2 \\ +6.2651\alpha_d - 4.2815, \ \alpha \geq \alpha_d \end{cases} \quad (2)$$

From (2), the field ratio γ_p corresponding to the desired aspect ratio α_d can be determined. However, the fitted model will change due to different doses of nanoparticles used for generating the swarm, and ambient fluids. Therefore, we adopt a fuzzy logic controller (FLC) for the online compensation of the model error.

The input and the output of the FLC is the error between the desired aspect ratio and the actual aspect ratio of the

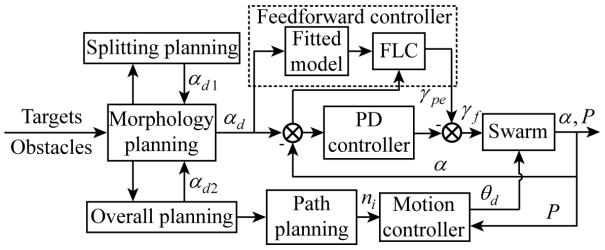

Fig. 5. The control diagram. The aspect ratio and position of the ribbon-like swarm is α and P, respectively. The desired aspect ratio for the controllable splitting of the swarm is α_{d1}, and the desired aspect ratio for the navigated locomotion of the swarm with a stable pattern is α_{d2}. The ith waypoint of the planned path and the desired moving direction for the navigated locomotion of the swarm is n_i and θ_d, respectively.

swarm e, and the control variable $\Delta\gamma_p$ to compensate the model error, respectively. Based on experimental data and human experiences, the membership functions of the input and output variables are obtained. In this work, the membership functions of the input and output variables are set the same, which are shown in Fig. 4(b). By adding the control variable $\Delta\gamma_p$, and the field ratio γ_p obtained from the fitted model, the output of the feedforward controller γ_{pe} can be expressed as:

$$\gamma_{pe} = \begin{cases} \gamma_p + \Delta\gamma_p(k), & e > e_t \\ \gamma_p + \Delta\gamma_p(k-1), & e \le e_t \end{cases} \tag{3}$$

where e_t is the threshold used to activate the online compensation for the model error. When $e > e_t$, γ_{pe} is determined by both the fitted model and the FLC. If $e \le e_t$, γ_{pe} is sufficiently accurate to keep the error within a controllable range, and γ_{pe} will keep the same as the value at the previous moment. In this case, the PD controller will dominate the control process to further decrease the error, and increase the robust of the morphology controller. The PD controller can be expressed as:

$$\Delta\gamma(k) = K_P e(k) + K_D\left[e(k) - e(k-1)\right] \tag{4}$$

Finally, the output of the morphology controller that combines the feedforward controller and the PD controller γ_f can be expressed as:

$$\gamma_f = \gamma_{pe} + \Delta\gamma(k) \tag{5}$$

Using the proposed morphology controller, the aspect ratio of the ribbon-like swarm can be kept within a desired range. In this case, by controlling the aspect ratio of the swarm at a small value, the locomotion of the swarm with a stable pattern can be maintained. The splitting of the swarms can also be controlled more precisely, since the aspect ratio of the swarm is kept within a specific range based on the morphology controller.

B. Control diagram

The control diagram for the automatic navigation of the ribbon-like swarm is shown in Fig. 5. The morphology planning of the ribbon-like swarm contains two sections, i.e., the splitting planning and the overall planning. The

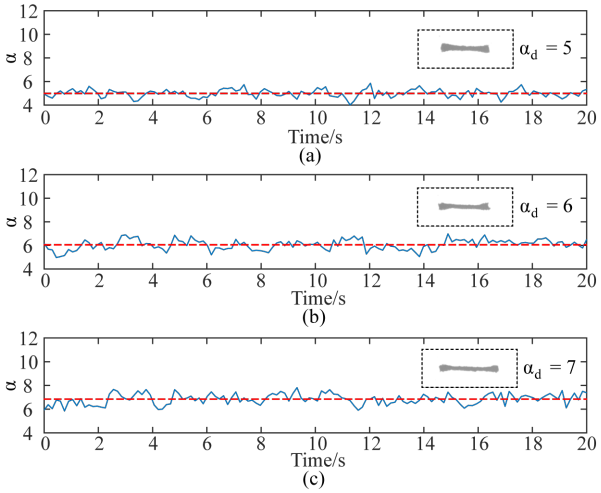

Fig. 6. The experimental results of controlling the aspect ratio of a ribbon-like swarm α using the morphology controller. The red line represents the average aspect ratio of the ribbon-like swarm during the control process. (a) The experimental results when the desired aspect ratio of the ribbon-like swarm α_d is 5. (b) The experimental results when the desired aspect ratio of the ribbon-like swarm α_d is 6. (c) The experimental results when the desired aspect ratio of the ribbon-like swarm α_d is 7.

splitting planning is designed for the controllable splitting of the swarm. In the spitting planning, based on the number of the targets, the number of the swarms after splitting is determined, and the corresponding desired aspect ratio of the swarm before splitting α_{d1} is obtained, using the theory mentioned in Section IV-B. The overall planning is designed for the navigated locomotion of the ribbon-like swarm, and the desired aspect ratio to maintain the stable pattern of the swarm is α_{d2}. In addition, to control the swarm to perform locomotion while passing obstacles in the environment, the path planning is adopted. The ith waypoint of the planned path is n_i, and the waypoint acts as a phased target for the navigation of the swarm. The position of n_i, i.e., $[P_{xi}, P_{yi}]^T$, is input to the motion controller, and the desired moving direction of the ribbon-like swarm θ_d can be expressed as:

$$\theta_d = \arctan\left(\frac{P_{yi} - P_y}{P_{xi} - P_x}\right) \tag{6}$$

where $P = [P_x, P_y]^T$ is the position of the swarm.

The desired aspect ratio α_d of the ribbon-like swarm is α_{d1} for controllable splitting of it, and α_{d2} for its locomotion with a stable pattern, respectively. The desired aspect ratio α_d is then input to the feedforward controller to obtain the predefined control input γ_{pe}, and the aspect ratio of the swarm α is input to the PD controller and the FLC as the feedback. Finally, the output of the morphology controller γ_f is obtained, and the aspect ratio of the swarm can be controlled within a desired range to realize the locomotion with a stable pattern, and controllable splitting.

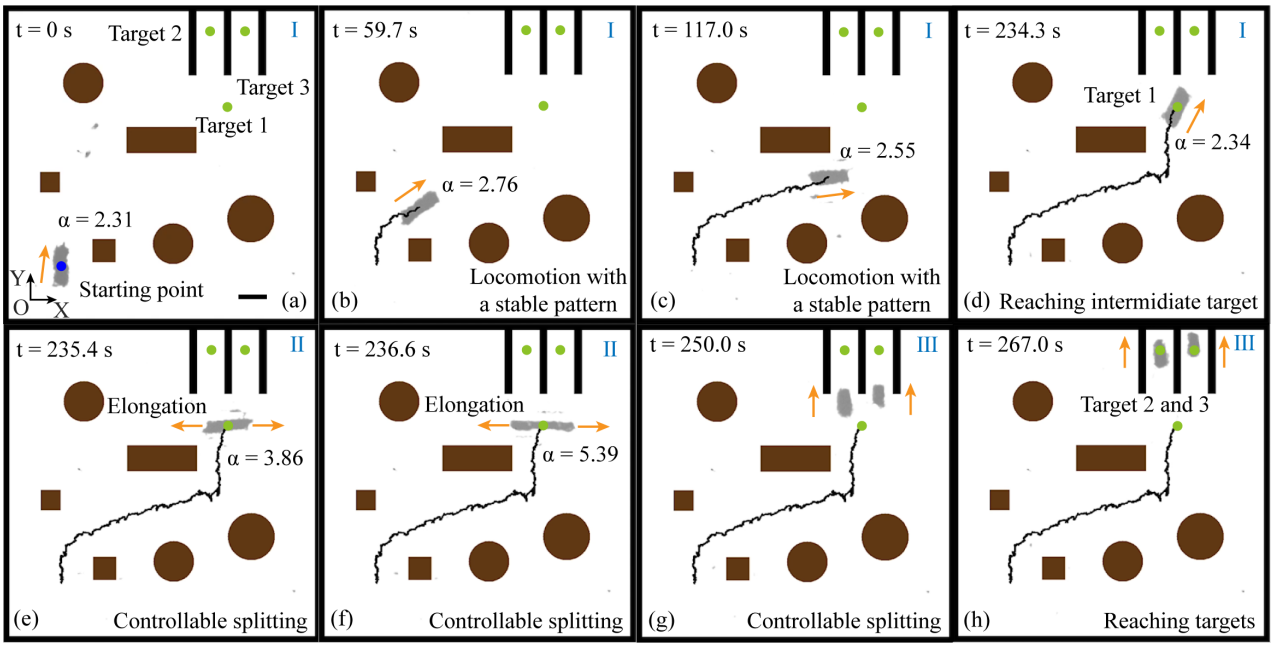

Fig. 7. The experimental results of navigated locomotion and controllable splitting of a ribbon-like swarm. The brown circles and rectangles represent the obstacles. The blue dot and the green dots indicate the starting point and the targets, respectively. The black denotes are the moving path of the ribbon-like swarm. The orange arrows in (a) - (d) and (g) – (h) represent the moving direction of the swarm, and the orange arrows in (e) and (f) denote the elongation direction of the swarm. The three states of the ribbon-like swarm are represented by I - III. The scale bar is 500 μm.

VI. Experimental Results

A. Experimental results of morphology control of a ribbon-like swarm

The experimental results of controlling the aspect ratio of a ribbon-like swarm α using the morphology controller are shown in Fig. 6. The control results when the desired aspect ratio of the ribbon-like swarm α_d is 5, 6, and 7 are shown in Fig. 6(a), Fig. 6(b), and Fig. 6(c), respectively. The average control error is 0.257, 0.355, and 0.386, when the desired aspect ratio α_d is 5, 6, and 7, respectively. The control results validate the effectiveness of the proposed morphology controller.

B. Navigated locomotion and controllable splitting of a ribbon-like swarm

The experimental results of navigated locomotion and controllable splitting of a ribbon-like swarm are shown in Fig. 7. There are three states of the ribbon-like swarm during the whole process. In State I, the swarm is performing locomotion with a stable pattern, when the aspect ratio α is small, as shown in Fig. 7(a) – Fig. 7(d). In State II, the swarm is performing elongation to prepare for the controllable splitting, as shown in Fig. 7(e) and Fig. 7(f). In State III, the double subswarms after splitting are performing locomotion with stable patterns to reach the two targets simultaneously, as shown in Fig. 7(g) and Fig. 7(h).

The ribbon-like swarm locates at the starting point at t = 0 s, as shown in Fig. 7(a). Subsequently, it moves along the planned path to approach the intermediate target, i.e., target 1. The planned path is generated using Fast marching tree algorithm (FMT*) [26]. The swarm can avoid the obstacle by following the planned path with a stable pattern, as shown in Fig. 7(b) and Fig. 7(c). Using the morphology controller mentioned in Section V-A, the aspect ratio of the swarm α is kept smaller than 3 in order to ensure the locomotion of the swarm with a stable pattern, as shown in Fig. 7(a) – Fig. 7(d). The swarm reaches the target 1 at t = 234.3 s, as shown in Fig. 7(d). When the swarm locates at the target 1, it will perform elongation to obtain a larger aspect ratio α for the controllable splitting, as shown in Fig. 7(e). At t = 236.6 s, the swarm finishes the elongation and starts performing controllable splitting by suddenly changing its moving direction from 0 degree to 90 degree. Before splitting, the aspect ratio of the swarm α is controlled at 5.39 using the morphology controller, as shown in Fig. 7(f). In this case, the number of the swarms after splitting will be 2 based on the theory mentioned in Section IV-B. After splitting, two subswarms are obtained, and the double subswarms move upward to approach two predefined targets, as shown in Fig. 7(g). At t = 267 s, the double subswarms reach the two predefined targets, indicating the navigation of the ribbon-like swarm is finished, as shown in Fig. 7(h). The experimental results of navigated locomotion and controllable splitting of a ribbon-like swarm validate the effectiveness of our proposed control strategy. The whole process is also demonstrated in the supplementary video.

VII. Conclusion

In this work, we present a control strategy to navigate a ribbon-like swarm to perform locomotion with a stable pattern while avoiding obstacles, and perform controllable splitting into double subswarms to reach two targets simul-

taneously. The two different behaviors of the ribbon-like swarm, i.e., locomotion with a stable pattern and controllable splitting, are firstly investigated. The two behaviors of the swarm is realized based on different aspect ratio of the swarm. Subsequently, a morphology controller is developed to keep the aspect ratio of the ribbon-like swarm within a desired range. The morphology controller consists of a feedforward controller and a PD controller. The feedforward controller contains a fitted model, and a fuzzy logic controller for online compensation of the model error. We subsequently propose a control strategy that combines the morphology planning, morphology controller, path planning, and motion controller of the ribbon-like swarm. Using the proposed control strategy, the ribbon-like swarm can follow the desired path with a stable pattern while passing obstacles, and perform controllable splitting into double subswarms to reach the two predefined targets simultaneously. This work focuses on the automatic navigation of microswarms based on morphology and motion control, and sheds light on multi-target delivery using microswarms in complicated environments.

REFERENCES

[1] B. J. Nelson, I. K. Kaliakatsos, and J. J. Abbott, "Microrobots for minimally invasive medicine," *Annual review of biomedical engineering*, vol. 12, pp. 55–85, 2010.

[2] M. Sitti, H. Ceylan, W. Hu, J. Giltinan, M. Turan, S. Yim, and E. Diller, "Biomedical applications of untethered mobile milli/microrobots," *Proceedings of the IEEE*, vol. 103, no. 2, pp. 205–224, 2015.

[3] X. Yan, Q. Zhou, M. Vincent, Y. Deng, J. Yu, J. Xu, T. Xu, T. Tang, L. Bian, Y.-X. J. Wang *et al.*, "Multifunctional biohybrid magnetite microrobots for imaging-guided therapy," *Science robotics*, vol. 2, no. 12, p. eaaq1155, 2017.

[4] J. Law, X. Wang, M. Luo, L. Xin, X. Du, W. Dou, T. Wang, G. Shan, Y. Wang, P. Song *et al.*, "Microrobotic swarms for selective embolization," *Science Advances*, vol. 8, no. 29, p. eabm5752, 2022.

[5] B. Wang, K. Kostarelos, B. J. Nelson, and L. Zhang, "Trends in micro-/nanorobotics: materials development, actuation, localization, and system integration for biomedical applications," *Advanced Materials*, vol. 33, no. 4, p. 2002047, 2021.

[6] W. Hu, G. Z. Lum, M. Mastrangeli, and M. Sitti, "Small-scale soft-bodied robot with multimodal locomotion," *Nature*, vol. 554, no. 7690, pp. 81–85, 2018.

[7] Y. Wang, X. Du, H. Zhang, Q. Zou, J. Law, and J. Yu, "Amphibious miniature soft jumping robot with on-demand in-flight maneuver," *Advanced Science*, p. 2207493, 2023.

[8] L. Yang, M. Sun, M. Zhang, and L. Zhang, "Multimodal motion control of soft ferrofluid robot with environment and task adaptability," *IEEE/ASME Transactions on Mechatronics*, 2023.

[9] Y. Dong, L. Wang, V. Iacovacci, X. Wang, L. Zhang, and B. J. Nelson, "Magnetic helical micro-/nanomachines: Recent progress and perspective," *Matter*, vol. 5, no. 1, pp. 77–109, 2022.

[10] X. Wu, J. Liu, C. Huang, M. Su, and T. Xu, "3-d path following of helical microswimmers with an adaptive orientation compensation model," *IEEE Transactions on Automation Science and Engineering*, vol. 17, no. 2, pp. 823–832, 2019.

[11] Y. Hou, H. Wang, S. Zhong, Y. Qiu, Q. Shi, T. Sun, Q. Huang, and T. Fukuda, "Design and control of a surface-dimple-optimized helical microdrill for motions in high-viscosity fluids," *IEEE/ASME Transactions on Mechatronics*, vol. 28, no. 1, pp. 429–439, 2022.

[12] V. Magdanz, I. S. Khalil, J. Simmchen, G. P. Furtado, S. Mohanty, J. Gebauer, H. Xu, A. Klingner, A. Aziz, M. Medina-Sánchez *et al.*, "Ironsperm: Sperm-templated soft magnetic microrobots," *Science advances*, vol. 6, no. 28, p. eaba5855, 2020.

[13] M. Li, J. Wu, D. Lin, J. Yang, N. Jiao, Y. Wang, and L. Liu, "A diatom-based biohybrid microrobot with a high drug-loading capacity and ph-sensitive drug release for target therapy," *Acta Biomaterialia*, vol. 154, pp. 443–453, 2022.

[14] H. Zhang, Z. Li, C. Gao, X. Fan, Y. Pang, T. Li, Z. Wu, H. Xie, and Q. He, "Dual-responsive biohybrid neutrobots for active target delivery," *Science Robotics*, vol. 6, no. 52, p. eaaz9519, 2021.

[15] J. Law, J. Yu, W. Tang, Z. Gong, X. Wang, and Y. Sun, "Micro/nanorobotic swarms: from fundamentals to functionalities," *ACS nano*, vol. 17, no. 14, pp. 12 971–12 999, 2023.

[16] J. Law, H. Chen, Y. Wang, J. Yu, and Y. Sun, "Gravity-resisting colloidal collectives," *Science Advances*, vol. 8, no. 46, p. eade3161, 2022.

[17] J. Yu, L. Yang, and L. Zhang, "Pattern generation and motion control of a vortex-like paramagnetic nanoparticle swarm," *The International Journal of Robotics Research*, vol. 37, no. 8, pp. 912–930, 2018.

[18] L. Yang, Y. Zhang, Q. Wang, K.-F. Chan, and L. Zhang, "Automated control of magnetic spore-based microrobot using fluorescence imaging for targeted delivery with cellular resolution," *IEEE Transactions on Automation Science and Engineering*, vol. 17, no. 1, pp. 490–501, 2019.

[19] J. Liu, X. Wu, C. Huang, L. Manamanchaiyaporn, W. Shang, X. Yan, and T. Xu, "3-d autonomous manipulation system of helical microswimmers with online compensation update," *IEEE Transactions on Automation Science and Engineering*, vol. 18, no. 3, pp. 1380–1391, 2020.

[20] T. Li, X. Chang, Z. Wu, J. Li, G. Shao, X. Deng, J. Qiu, B. Guo, G. Zhang, Q. He *et al.*, "Autonomous collision-free navigation of microvehicles in complex and dynamically changing environments," *Acs Nano*, vol. 11, no. 9, pp. 9268–9275, 2017.

[21] L. Yang, J. Yu, and L. Zhang, "Statistics-based automated control for a swarm of paramagnetic nanoparticles in 2-d space," *IEEE Transactions on Robotics*, vol. 36, no. 1, pp. 254–270, 2019.

[22] Y. Liu, H. Chen, Q. Zou, X. Du, Y. Wang, and J. Yu, "Automatic navigation of microswarms for dynamic obstacle avoidance," *IEEE Transactions on Robotics*, 2023.

[23] Q. Zou, X. Du, Y. Liu, H. Chen, Y. Wang, and J. Yu, "Dynamic path planning and motion control of microrobotic swarms for mobile target tracking," *IEEE Transactions on Automation Science and Engineering*, 2022.

[24] J. Yu, L. Yang, X. Du, H. Chen, T. Xu, and L. Zhang, "Adaptive pattern and motion control of magnetic microrobotic swarms," *IEEE Transactions on Robotics*, vol. 38, no. 3, pp. 1552–1570, 2021.

[25] J. Yu, B. Wang, X. Du, Q. Wang, and L. Zhang, "Ultra-extensible ribbon-like magnetic microswarm," *Nature communications*, vol. 9, no. 1, p. 3260, 2018.

[26] L. Janson, E. Schmerling, A. Clark, and M. Pavone, "Fast marching tree: A fast marching sampling-based method for optimal motion planning in many dimensions," *The International journal of robotics research*, vol. 34, no. 7, pp. 883–921, 2015.